Date of publication xxxx 00, 0000, date of current version xxxx 00, 0000.

Digital Object Identifier

On the Energy Efficiency of Interference Alignment in the K-User Interference Channel

XIAQING MIAO[1], SHAOSHI YANG[2] (SENIOR MEMBER, IEEE), CHANGHONG WANG[1], SHUAI WANG[1] AND LAJOS HANZO[3] (Fellow, IEEE)

[1]School of Information and Electronics, Beijing Institute of Technology, Beijing 100081, China
[2]School of Information and Communication Engineering, Beijing University of Posts and Telecommunications, Beijing 100876, China
[3]School of Electronics and Computer Science, University of Southampton, Southampton SO17 1BJ, U.K.

Corresponding author: Shaoshi Yang (e-mail: shaoshi.yang@ieee.org).

L. Hanzo would like to acknowledge the financial support of the Engineering and Physical Sciences Research Council projects EP/Noo4558/1, EP/PO34284/1, COALESCE, of the Royal Society's Global Challenges Research Fund Grant as well as of the European Research Council's Advanced Fellow Grant QuantCom.

ABSTRACT Interference alignment (IA) is regarded as an important physical-layer interference management technique. Most research contributions on IA were focused on the analysis of its achievable spectral efficiency, either from the degrees of freedom or from the capacity perspective. Meanwhile, high energy-efficiency (EE) has become a key requirement for next-generation wireless communications. Hence, we focus our attention on the EE of IA in the fully connected K-user interference channel, where each user has either a single antenna or multiple antennas. We consider both perfect and imperfect channel state information scenarios. New insights into the achievable EE of IA are obtained by investigating the impact of different precoding matrices, the number of users, the number of antennas, symbol extension values, channel estimation accuracy, total transmit power and power allocation schemes. In particular, we demonstrate that in the single-antenna-user case, the IA schemes relying on unequal power allocation achieves higher EE than their equal power allocation counterparts. However, in the scenario where each user is equipped with multiple antennas, equal power allocation achieves higher EE than unequal power allocation for IA. Furthermore, using non-uniform precoding-matrix-generating vector $\boldsymbol{w}$ is not necessarily beneficial for improving the achievable EE of IA. We also find that the EE performance of IA with smaller symbol extension values is higher than that with larger symbol extension values, the achievable EE of IA decays with the increase of the total transmit power, the EE performance of IA degrades as the channel estimation accuracy becomes low, and that having a larger number of transmit/receive antennas on each user achieves a higher EE in IA.

INDEX TERMS Interference alignment, energy efficiency, green communications, interference channel, imperfect channel state information

I. INTRODUCTION

INTERFERENCE alignment (IA) has attracted substantial research interests during the past decade [1]–[10], since it sheds light on a promising avenue for approaching the capacity of interference-limited wireless networks. Considering the fully connected K-user interference channel composed of K pairs of transmitters and receivers, Jafar *et al.* [5] showed that $K/2$ degrees of freedom (DoF) is achievable by IA under certain strict conditions, where the DoF is also known as the capacity pre-log characterizing the multiplexing gain [11]. By contrast, the DoF of the conventional orthogonal multi-access based interference management schemes is 1, which is much lower than $K/2$ when K is high.

Meanwhile, increasing economical and environmental concerns are calling for a significant reduction of the carbon-footprint of the telecom industry. As a result, energy efficiency (EE) has become an important design metric of next-generation wireless communication systems [12]–[19]. However, most existing research contributions on IA were focused on the analysis and improvement of its spectral

efficiency (SE) in various interference-limited systems [4]–[10], by invoking either the DoF or the capacity as the performance metric. By contrast, how to understand IA from the fundamental EE perspective remains rarely documented. There are a few treatises related to the EE of IA indeed. For example, Yoon *et al.* [20] proposed a distributed opportunistic IA scheme, which was shown to be more energy-efficient than the opportunistic IA. Additionally, adaptive power allocation and transmission mode (sleeping or active) selection schemes were studied in [21] for optimizing the achievable EE of the K-user interference network that uses IA. In [22] the normalized-EE maximization problem was solved in a multi-cell multi-input–multi-output orthogonal frequency-division multi-access (MIMO-OFDMA) system that uses IA, where it was shown that the partial-IA scheme is more energy-efficient than the full-IA scheme. The authors of [23] proposed a new network architecture based on EE maximization for multi-cell MIMO interfering broadcast channels using IA, and different IA schemes were employed for the high and moderate signal-to-noise ratio (SNR) regions. These contributions provided valuable insights into the EE of several sophisticated systems, where different variants of IA were invoked. However, in these systems the IA schemes are entangled with other techniques, which limits our understanding of the EE of IA itself.

Owing to the importance of both IA and EE, the EE of IA techniques deserves a deeper and more comprehensive investigation. It is well-known that the IA technique was originally conceived for the fully connected K-user interference channel [5], where all the users are equipped either with a single antenna or with multiple antennas. For the IA schemes of [5], the transmitters have to know the perfect global channel state information (CSI) for constructing the precoding matrices. However, obtaining the global CSI is challenging. Moreover, the CSI obtained at transmitters of a practical system is usually imperfect due to the time-varying nature of channels, the estimation error, the quantization error, the feedback error, and so forth.

In this paper, we study the EE performance of representative IA schemes in the context of the fundamental fully connected K-user interference channel, for which the IA technique was originally invented. Our novel contributions are summarized as follows.

- Closed-form EE expressions of the IA schemes considered are formulated under both the perfect and imperfect CSI assumptions, and in both the single-antenna and multi-antenna systems.
- In contrast to [5], [24], where the equal power allocation strategy and the precoding matrices determined by the all-one column vector $\boldsymbol{w} = \mathbf{1}$ are used, we demonstrate that in the single-antenna-user case, the variant IA schemes relying on unequal power allocation achieves higher EE than their equal power allocation counterparts. However, in the scenario where each user is equipped with multiple antennas, equal power allocation achieves higher EE than unequal power allocation for IA. Furthermore, using non-uniform precoding-matrix-generating vector $\boldsymbol{w}$ is not necessarily beneficial for improving the achievable EE of IA.
- We find that in the symbol-extension based IA schemes, when the symbol extension values become sufficiently high, the "effective channel" at a given receiver becomes ill-conditioned and almost singular. This phenomenon will cause numerical accuracy and stability problems when using the zero forcing (ZF) receiver. We conceive a channel truncation method to address this issue.
- We analyze the computational complexity of the IA schemes considered, and quantify how the number of users, the number of antennas, the symbol extension values, the channel estimation accuracy, the total transmit power and the power allocation schemes influence the EE of the IA schemes considered.

The rest of this paper is organized as follows. The EE of IA in the K-user interference channel with single-antenna nodes and multi-antenna nodes is theoretically studied in Section II and Section III, respectively. The computational complexity of the IA schemes considered is analyzed in Section IV. Our simulation results and discussions are presented in Section V. Finally, our conclusions are offered in Section VI.

Notations: We use boldface uppercase and lowercase letters to denote matrices and vectors, respectively. $\boldsymbol{I}_n$ represents the identity matrix of size $n \times n$. $(\cdot)^H$ and $|\cdot|$ refer to the conjugate transpose and the determinant of a matrix, respectively.

II. THE EE OF IA IN THE SINGLE-ANTENNA K-USER INTERFERENCE CHANNEL

A. THE CANONICAL IA SCHEME

We first consider an interference channel having K single-antenna transmitters and K single-antenna receivers. For clarity, the canonical IA scheme of [5] in the single-antenna case is illustrated in Fig. 1, which is described in detail below.

Each transmitter, such as the transmitter j, is supposed to send information only to its associated unique receiver. The output at the kth receiver during the tth channel use is given as follows:

$$y_k(t) = \sum_{j=1}^{K} h_{kj}(t)x_j(t) + z_k(t), \tag{1}$$

where $j, k = 1, 2, \cdots, K$ is the user index; the integer t represents the time slot index, the frequency slot index, or the time-frequency block index; $x_j(t)$ denotes the input signal of the jth transmitter; and $h_{kj}(t)$ is the channel fading coefficient from transmitter j to receiver k during the tth channel use. To avoid degenerate channel conditions (e.g., the rank-deficient channel matrix, or the channel matrix that has zero or infinity entries), we assume that $h_{kj}(t)$ is constituted by independently and identically distributed (i.i.d.) random variables drawn from a continuous distribution, e.g., $\mathcal{CN}(0, 1)$, and has to satisfy: $0 < h_{\min} \leq |h_{kj}| \leq h_{\max} < \infty$. Additionally, $z_k(t) \sim \mathcal{CN}(0, 1)$ represents the additive white

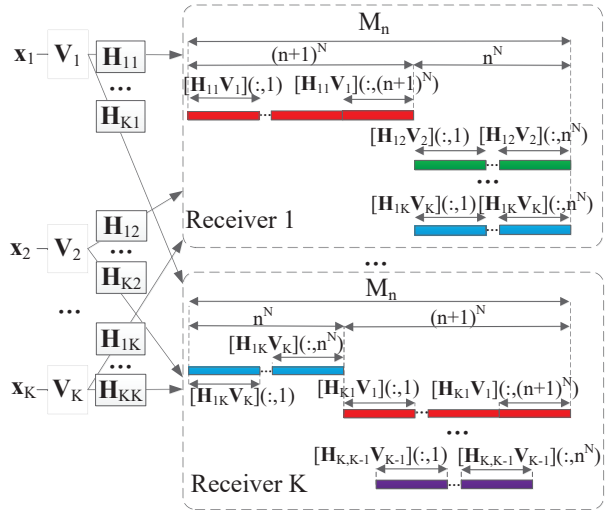

FIGURE 1. The IA scheme [5] with single-antenna nodes.

Gaussian noise (AWGN) at the kth receiver, and all the noise terms across the receivers are assumed to be independent.

In the IA scheme of [5], upon defining

$$N = (K-1)(K-2) - 1, \tag{2}$$

it was shown that $[(n+1)^N + (K-1)n^N]$ DoF is achievable over a symbol extension of

$$M_e = (n+1)^N + n^N \tag{3}$$

time slots in the time-varying channel that has no inter-symbol interference. More specifically, in this context, the first transmitter achieves $(n+1)^N$ DoF, while each of the other transmitters achieves n^N DoF, by transmitting the information-bearing signals with the help of their judiciously designed individual precoding vectors/matrices. Here n can be any positive integer. It is also assumed that all the transmitted signals arrive at the receivers simultaneously. Based on this multi-symbol extended channel, the signal vector at the kth receiver is expressed as

$$\boldsymbol{y}_k = \boldsymbol{H}_{kk}\boldsymbol{V}_k\boldsymbol{x}_k + \sum_{j\neq k}^{K} \boldsymbol{H}_{kj}\boldsymbol{V}_j\boldsymbol{x}_j + \boldsymbol{z}_k, \tag{4}$$

where $\boldsymbol{y}_k \in \mathbb{C}^{M_e\times 1}$, and $\boldsymbol{H}_{kj}$ is an $M_e \times M_e$ diagonal matrix representing the CSI from transmitter j to receiver k over the M_e-symbol extension of the channel, as shown in (5). In this paper, we consider both the perfect and the imperfect CSI scenarios. Additionally, $\boldsymbol{x}_1 \in \mathbb{C}^{(n+1)^N\times 1}$ represents the input signal of the first transmitter, while $\boldsymbol{x}_j \in \mathbb{C}^{n^N\times 1}$ $(j = 2,3,\cdots,K)$ is the input signal of the jth transmitter. Moreover, it is assumed that $\boldsymbol{x}_1 \sim \mathcal{CN}(\boldsymbol{0}, P_1\boldsymbol{I}_{(n+1)^N})$ and $\boldsymbol{x}_j$ $(j = 2,3,\cdots,K)$ obeys $\mathcal{CN}(\boldsymbol{0}, P_j\boldsymbol{I}_{n^N})$, where P_j denotes the power of each transmitter. $\boldsymbol{V}_1 \in \mathbb{C}^{M_e\times(n+1)^N}$ and $\boldsymbol{V}_j \in \mathbb{C}^{M_e\times n^N}$ $(j = 2,3,\cdots,K)$ are the precoding matrices invoked at the individual transmitters, respectively. Finally, $\boldsymbol{z}_k \in \mathbb{C}^{M_e\times 1}$ represents the AWGN, i.e. $\boldsymbol{z}_k \sim \mathcal{CN}(\boldsymbol{0}, \boldsymbol{I}_{M_e})$.

To align the interference at each of the receivers, the precoding matrices are constructed in [5] as follows. The set of column vectors of $\boldsymbol{V}_1$ is chosen to be equal to the set $\mathbb{V}_1$, which has $(n+1)^N$ elements and is defined as

$$\mathbb{V}_1 = \left\{ \left(\prod_{m,k\in\{2,3,\ldots K\}, m\neq k, (m,k)\neq(2,3)} \left(\boldsymbol{T}_k^{[m]}\right)^{\alpha_{mk}} \right) \boldsymbol{w} : \forall \alpha_{mk} \in \{0,1,2,\ldots,n\} \right\}; \tag{6}$$

the other precoding matrices are determined using

$$\boldsymbol{V}_j = \boldsymbol{S}^{[j]}\boldsymbol{B}, \quad j = 2,3,\ldots,K, \tag{7}$$

where we have

$$\boldsymbol{S}^{[j]} = (\boldsymbol{H}_{1j})^{-1}\boldsymbol{H}_{13}(\boldsymbol{H}_{23})^{-1}\boldsymbol{H}_{21}, \quad j = 2,3,\ldots,K, \tag{8}$$

$$\boldsymbol{T}_j^{[i]} = (\boldsymbol{H}_{i1})^{-1}\boldsymbol{H}_{ij}\boldsymbol{S}^{[j]}, \quad i,j = 2,3,\ldots,K, j\neq i, \tag{9}$$

and the set of column vectors of $\boldsymbol{B}$ is chosen to be equal to the set $\mathbb{B}$, which has n^N elements and is defined as

$$\mathbb{B} = \left\{ \left(\prod_{m,k\in\{2,3,\ldots K\}, m\neq k, (m,k)\neq(2,3)} \left(\boldsymbol{T}_k^{[m]}\right)^{\alpha_{mk}} \right) \boldsymbol{w} : \forall \alpha_{mk} \in \{0,1,2,\ldots,n-1\} \right\}. \tag{10}$$

Herein $\boldsymbol{w}$ is an $M_e \times 1$ all-one column vector.

Once the interference is aligned at the receivers, the following constraints are satisfied:

$$\boldsymbol{H}_{12}\boldsymbol{V}_2 = \boldsymbol{H}_{13}\boldsymbol{V}_3 = \cdots = \boldsymbol{H}_{1K}\boldsymbol{V}_K, \tag{11}$$

$$\boldsymbol{H}_{ij}\boldsymbol{V}_j \prec \boldsymbol{H}_{i1}\boldsymbol{V}_1, \quad j \notin \{1,i\}, \tag{12}$$

where we have $i,j = 2,3,\cdots,K$, and the operator "$\prec$" represents that the set of column vectors of the left-hand matrix is a subset of the set of column vectors composing the right-hand matrix.

B. A PRECODING-MATRIX OPTIMIZED IA SCHEME

The achievable DoF of the IA scheme in [5] is asymptotically optimal. To attain a higher DoF than the scheme of [5] at any given number of channel realizations, an IA scheme, which is capable of achieving the same DoF of [5] with smaller symbol extension values, was designed from the perspective of signal space for the case of $K \geq 3$ based on an improved precoding matrix design criterion in [24]. Specifically, in [24] the length of symbol extension is given by

$$M_e = \binom{n^*+N+1}{N} + \binom{n^*+N}{N}, \tag{13}$$

where we have $N = (K-1)(K-2)-1$. Additionally, for given $q \neq 1, p \neq q$, by defining $\boldsymbol{T}_j^{*[i]} = (\boldsymbol{H}_{i1})^{-1}\boldsymbol{H}_{ij}(\boldsymbol{H}_{1j})^{-1}\boldsymbol{H}_{1q}, i,j = 2,3,\ldots,K, j\neq i$, the set of column vectors of the precoding matrix $\boldsymbol{V}_1^*$ at the first transmitter is chosen to be the set $\mathbb{V}_1^*$, which has $\binom{n^*+N+1}{N}$

$$\boldsymbol{H}_{kj} = \begin{bmatrix} h_{kj}(M_e(t-1)+1) & 0 & \cdots & 0 \\ 0 & h_{kj}(M_e(t-1)+2) & \cdots & 0 \\ \vdots & \cdots & \ddots & \vdots \\ 0 & 0 & \cdots & h_{kj}(M_e t) \end{bmatrix}. \tag{5}$$

$$\mathbb{V}_1^* = \left\{ \left(\prod_{m,k\in\{2,3,\ldots K\}, m\neq k, (m,k)\neq(p,q)} \left((\boldsymbol{T}_q^{*[p]})^{-1} \boldsymbol{T}_k^{*[m]} \right)^{\alpha_{mk}} \right) \boldsymbol{w} : \sum_{m,k\in\{2,3,\ldots K\}, m\neq k, (m,k)\neq(p,q)} \alpha_{mk} \leq n^* + 1 \right\}; \tag{14}$$

$$\mathbb{V}_q^* = \left\{ (\boldsymbol{T}_q^{*[p]})^{-1} \left(\prod_{m,k\in\{2,3,\ldots K\}, m\neq k, (m,k)\neq(p,q)} \left((\boldsymbol{T}_q^{*[p]})^{-1} \boldsymbol{T}_k^{*[m]} \right)^{\alpha_{mk}} \right) \boldsymbol{w} : \sum_{m,k\in\{2,3,\ldots K\}, m\neq k, (m,k)\neq(p,q)} \alpha_{mk} \leq n^* \right\}. \tag{15}$$

elements and is defined as (14). Furthermore, the set of column vectors of the precoding matrix $\boldsymbol{V}_q^*$ at the qth transmitter is chosen to be the set $\mathbb{V}_q^*$, which has $\binom{n^*+N}{N}$ elements and is defined as (15). Here n^* can be any nonnegative integer. The other precoding matrices are determined using

$$\boldsymbol{V}_k^* = \boldsymbol{H}_{1k}^{-1} \boldsymbol{H}_{1q} \boldsymbol{V}_q^*, \tag{16}$$

where we have $k \in \{2, 3, \ldots, K\}, k \neq q$.

C. THE EE OF IA WITH PERFECT CSI

With the IA scheme of [5] in mind, we aim to design the precoding and receiving matrices for ensuring that the following conditions are satisfied: when the set of channel matrices and the set of precoding matrices are assumed to be entirely and perfectly known to all transmitters and receivers, the kth receiver's interference subspace spanned by the column vectors of $\boldsymbol{H}_{kj}\boldsymbol{V}_j$ $(\forall j \neq k)$ can be eliminated by using the ZF technique at the kth receiver. We normalize the power of $\boldsymbol{V}_k$ to 1. Hence we have $\frac{1}{M_e}\mathrm{Tr}\left(\boldsymbol{V}_k\boldsymbol{V}_k^H\right) = 1, \forall k \in \{1, \ldots, K\}$.

For the first receiver, the interference arriving from transmitters $2, 3, \ldots, K$ can be aligned according to: $\boldsymbol{H}_{12}\boldsymbol{V}_2 = \boldsymbol{H}_{13}\boldsymbol{V}_3 = \cdots = \boldsymbol{H}_{1K}\boldsymbol{V}_K$. Therefore, the ZF filtering matrix at the first receiver is formulated as follows:

$$\boldsymbol{W}_1^{\mathrm{ZF}} = \boldsymbol{\Psi}_1 \widetilde{\boldsymbol{H}}_1^{-1}, \tag{17}$$

where $\boldsymbol{\Psi}_1 = [\boldsymbol{I}_{d_1}, \boldsymbol{0}_{d_1\times(M_e-d_1)}]$ and $\widetilde{\boldsymbol{H}}_1 = [\boldsymbol{H}_{11}\boldsymbol{V}_1, \boldsymbol{H}_{12}\boldsymbol{V}_2]$, while $d_1 = (n+1)^N$ denotes the achieved DoF of the first transmitter.

For the other receivers $k \neq 1$, the condition $\boldsymbol{H}_{kj}\boldsymbol{V}_j \prec \boldsymbol{H}_{k1}\boldsymbol{V}_1, j \notin \{1, k\}$ is satisfied. Then the ZF filtering matrix associated with receiver k can be expressed as

$$\boldsymbol{W}_k^{\mathrm{ZF}} = \boldsymbol{\Psi}_k \widetilde{\boldsymbol{H}}_k^{-1}, \tag{18}$$

where $\boldsymbol{\Psi}_k = [\boldsymbol{I}_{d_k}, \boldsymbol{0}_{d_k\times(M_e-d_k)}]$ and $\widetilde{\boldsymbol{H}}_k = [\boldsymbol{H}_{kk}\boldsymbol{V}_k, \boldsymbol{H}_{k1}\boldsymbol{V}_1]$, while $d_k = n^N$ denotes the achieved DoF of the kth transmitter[1].

Applying the ZF receivers given by (17) and (18) to the received signal of (4) results in the following matrix-form SNR expression[2] at the receiver k:

$$\boldsymbol{\gamma}_k = \chi_k P_t \mathbb{E}\{\boldsymbol{\Theta}_k^{-1}\}, \tag{19}$$

where P_t denotes the total transmit power of all the transmitters, and $\chi_k = \frac{P_k}{P_t}$ represents the percentage of P_t that the kth transmitter's power dissipation P_k accounts for, which must satisfy: $\sum_{k=1}^{K} \chi_k = 1$. Finally, $\boldsymbol{\Theta}_k$ is defined as $\boldsymbol{\Psi}_k \widetilde{\boldsymbol{H}}_k^{-1} \boldsymbol{z}_k{}^{-1} \boldsymbol{z}_k (\widetilde{\boldsymbol{H}}_k^{-1})^H \boldsymbol{\Psi}_k^H$.

Then the individual rate at the kth receiver is formulated as

$$R_k = \log_2(|\boldsymbol{I}_{d_k} + \boldsymbol{\gamma}_k|) \tag{20}$$

[bits per symbol extension block]. The average sum rate achieved by the IA scheme [5] in the perfect CSI scenario is then given by

$$\bar{R} = \frac{1}{M_e} \sum_{k=1}^{K} R_k \tag{21}$$

[bits per channel use].

[1]We find that when the symbol extension values become sufficiently high, the channel $\widetilde{H}_k$ in (17) and (18) become ill-conditioned and almost singular, if its entries are not truncated properly. Consequently, in numerical calculations the ZF filtering matrix that requires the inverse operation at each receiver cannot be obtained with a sufficiently high accuracy. On the other hand, although the channel coefficients following $\mathcal{CN}(0,1)$ have a probability of taking any value, it is reasonable to truncate the extreme values that are far away from the mean zero, as it is well known that the probability of taking such values is very small. Therefore, to make the simulation results more accurate, we make such a truncated channel assumption as stated in Sec. II-A.

[2]This is a diagonal matrix, in which the M_e non-zero elements correspond to the SNR values associated with the M_e symbol extension.

Moreover, the total power dissipation of the system designed for communicating over an interference channel can be modeled as

$$P = P_t + P_c, \tag{22}$$

where P_c denotes the fixed circuit power consumption, and it significantly affects the system's EE performance.

As a result, the EE of the IA system considered is formulated as

$$\eta_{\text{EE}} = \frac{\bar{R}}{P}. \tag{23}$$

As far as the IA scheme of [24] is concerned, by replacing $\boldsymbol{V}_k$ in (17) and (18) with $\boldsymbol{V}_k^*$ of (14), (15) and (16), and using Equations (19) $\sim$ (23), a higher EE performance is achieved when $K \geq 4$,[3] as demonstrated in Sec. IV. Additionally, it should be noted that both the IA scheme of [5] and the IA scheme of [24] employ the uniform precoding-matrix-generating vector of $\boldsymbol{w} = \mathbf{1}$ and the equal power allocation scheme characterized by $\chi_k = 1/K$. By contrast, we propose to improve the EE performance of IA by using non-uniform precoding-matrix-generating vectors, where the elements of $\boldsymbol{w}$ are not all equal to one, as well as unequal power allocation, where χ_k can have different values for different k.

D. THE EE OF IA WITH IMPERFECT CSI

In realistic wireless environments, the perfect CSI is difficult to obtain at transceivers due to various factors, such as the time-varying nature of wireless channels, the channel estimation error, the quantization error and the feedback error/delay. Hence it is important to study the EE of IA in the imperfect CSI scenario, where the channel can be modeled as [25]

$$\boldsymbol{H}_{kj} = \sqrt{1-\beta^2}\widehat{\boldsymbol{H}}_{kj} + \beta \boldsymbol{E}_{kj}, \tag{24}$$

where the $M_e \times M_e$ diagonal matrix $\widehat{\boldsymbol{H}}_{kj}$ represents the estimated CSI available to network nodes, and the diagonal elements of $\boldsymbol{E}_{kj}$ are i.i.d Gaussian noise components. Each diagonal element of $\widehat{\boldsymbol{H}}_{kj}$ and $\boldsymbol{E}_{kj}$ obeys $\mathcal{CN}(0,1)$, and β controls the CSI accuracy. Substituting (24) into (4), the signal at the kth receiver can be expressed as

$$\boldsymbol{y}_k = \sqrt{1-\beta^2}\sum_{j=1}^{K}\widehat{\boldsymbol{H}}_{kj}\boldsymbol{V}_j\boldsymbol{x}_j + \beta\sum_{j=1}^{K}\boldsymbol{E}_{kj}\boldsymbol{V}_j\boldsymbol{x}_j + \boldsymbol{z}_k. \tag{25}$$

The second term on the right-hand side of (25) is the additional interference imposed by the channel uncertainty. Relying on (17) and (18), we have $\widehat{\boldsymbol{W}}_1^{\text{ZF}} = \boldsymbol{\Psi}_1\underline{\boldsymbol{H}}_1^{-1}$ and $\widehat{\boldsymbol{W}}_k^{\text{ZF}} = \boldsymbol{\Psi}_k\underline{\boldsymbol{H}}_k^{-1}, k \neq 1$, in which $\underline{\boldsymbol{H}}_1^{-1} = [\widehat{\boldsymbol{H}}_{11}\boldsymbol{V}_1, \widehat{\boldsymbol{H}}_{12}\boldsymbol{V}_2]$ and $\underline{\boldsymbol{H}}_k^{-1} = [\widehat{\boldsymbol{H}}_{kk}\boldsymbol{V}_k, \widehat{\boldsymbol{H}}_{k1}\boldsymbol{V}_1]$. Applying the ZF receiver formulations mentioned above to the received signal given by (25), the matrix-form signal-to-interference-plus-noise ratio (SINR) corresponding to M_e symbol extension at the kth receiver is written as

$$\boldsymbol{\gamma}_k' = \mathbb{E}\Big\{\frac{(1-\beta^2)\chi_k P_t}{\beta^2\sum_{j=1}^{K}\{\widehat{\boldsymbol{W}}_k^{\text{ZF}}\boldsymbol{E}_{kj}\boldsymbol{F}_j\boldsymbol{E}_{kj}^H(\widehat{\boldsymbol{W}}_k^{\text{ZF}})^H\} + \mathbb{E}\{\boldsymbol{\Theta}_k\}}\Big\}, \tag{26}$$

where $\boldsymbol{F}_j = \mathbb{E}\{\boldsymbol{V}_j\boldsymbol{x}_j\boldsymbol{x}_j^H\boldsymbol{V}_j^H\} = \chi_j P_t \boldsymbol{V}_j\boldsymbol{V}_j^H$. Thus (26) can be simplified as:

$$\begin{aligned}\boldsymbol{\gamma}_k' &= \frac{(1-\beta^2)\chi_k P_t}{\beta^2\sum_{j=1}^{K}\chi_j P_t\mathbb{E}\{\widehat{\boldsymbol{W}}_k^{\text{ZF}}\boldsymbol{E}_{kj}\boldsymbol{V}_j\boldsymbol{V}_j^H\boldsymbol{E}_{kj}^H(\widehat{\boldsymbol{W}}_k^{\text{ZF}})^H\} + \mathbb{E}\{\boldsymbol{\Theta}_k\}} \\ &= \frac{(1-\beta^2)\chi_k P_t}{\widehat{\boldsymbol{W}}_k^{\text{ZF}}\left(\beta^2\sum_{j=1}^{K}\chi_j P_t\boldsymbol{D}_j + \boldsymbol{I}_{d_{M_e}}\right)(\widehat{\boldsymbol{W}}_k^{\text{ZF}})^H},\end{aligned} \tag{27}$$

where $\boldsymbol{D}_j$ denotes the matrix composed of the diagonal elements of $\boldsymbol{V}_j\boldsymbol{V}_j^H$, and the EE expression in the imperfect CSI scenario is given by replacing $\boldsymbol{\gamma}_k$ of (19) with $\boldsymbol{\gamma}_k'$ of (27) and following Equations (20)$\sim$(23).

III. THE EE OF IA IN THE MULTI-ANTENNA K-USER INTERFERENCE CHANNEL

Let us further investigate the EE of the canonical IA scheme [5] for the K-user interference channel, where each node has $M > 1$ antennas. In this multi-antenna scenario, the closed-form EE expression is only available for $K \leq 3$, hence we assume $K = 3$ in the following derivations. It has been shown [5] that each transmitter achieves $M/2$ DoF when the inter-symbol interference is eliminated and the channel matrices are constant during each transmission period.

A. THE EE OF IA FOR EVEN-VALUED M

The IA scheme for even-valued M is illustrated in Fig. 2. More specifically, the signal received by the kth receiver can be written as

$$\boldsymbol{y}_k = \boldsymbol{H}_{k1}\boldsymbol{V}_1\boldsymbol{x}_1 + \boldsymbol{H}_{k2}\boldsymbol{V}_2\boldsymbol{x}_2 + \boldsymbol{H}_{k3}\boldsymbol{V}_3\boldsymbol{x}_3 + \boldsymbol{z}_k, \tag{28}$$

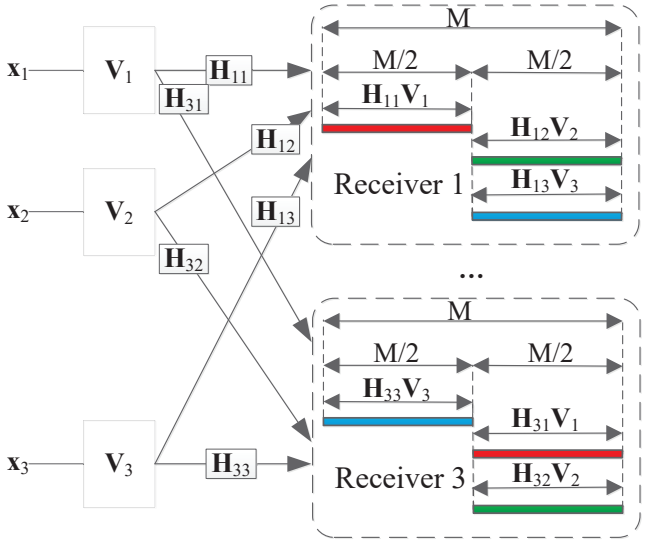

FIGURE 2. The IA scheme [5] where each node has an even number of multiple antennas.

[3]Because the transmit beamforming design criterion [24] attained higher sum DoF using shorter symbol extension when $K \geq 4$, $\boldsymbol{V}_k^*$ results in higher sum rate, as well as higher EE.

where $\boldsymbol{y}_k \in \mathbb{C}^{M\times 1}$, $\boldsymbol{H}_{kj}$ $(k,j \in \{1,2,3\})$ is an $M \times M$ matrix representing the CSI from transmitter j to receiver k, $\boldsymbol{V}_k \in \mathbb{C}^{M\times \frac{M}{2}}$ is the precoding matrix invoked by the individual transmitters, $\boldsymbol{x}_k \sim \mathcal{CN}(\boldsymbol{0}, P_k \boldsymbol{I}_{\frac{M}{2}})$, and $\boldsymbol{z}_k \in \mathbb{C}^{M\times 1}$ represents the AWGN, i.e. $\boldsymbol{z}_k \sim \mathcal{CN}(\boldsymbol{0}, \boldsymbol{I}_M)$.

To align the interference at each of the receivers, the following constraints must be satisfied:

$$\text{span}(\boldsymbol{H}_{12}\boldsymbol{V}_2) = \text{span}(\boldsymbol{H}_{13}\boldsymbol{V}_3), \tag{29}$$
$$\boldsymbol{H}_{21}\boldsymbol{V}_1 = \boldsymbol{H}_{23}\boldsymbol{V}_3, \tag{30}$$
$$\boldsymbol{H}_{31}\boldsymbol{V}_1 = \boldsymbol{H}_{32}\boldsymbol{V}_2, \tag{31}$$

where $\text{span}(\boldsymbol{A})$ represents the vector space spanned by the column vectors of matrix $\boldsymbol{A}$. Since $\boldsymbol{H}_{kj}$ has a full rank almost surely, the above equations can be equivalently written as

$$\text{span}(\boldsymbol{V}_1) = \text{span}(\boldsymbol{E}\boldsymbol{V}_1), \tag{32}$$
$$\boldsymbol{V}_2 = \boldsymbol{F}\boldsymbol{V}_1, \tag{33}$$
$$\boldsymbol{V}_3 = \boldsymbol{G}\boldsymbol{V}_1, \tag{34}$$

where

$$\boldsymbol{E} = (\boldsymbol{H}_{31})^{-1}\boldsymbol{H}_{32}(\boldsymbol{H}_{12})^{-1}\boldsymbol{H}_{13}(\boldsymbol{H}_{23})^{-1}\boldsymbol{H}_{21}, \tag{35}$$
$$\boldsymbol{F} = (\boldsymbol{H}_{32})^{-1}\boldsymbol{H}_{31}, \tag{36}$$
$$\boldsymbol{G} = (\boldsymbol{H}_{23})^{-1}\boldsymbol{H}_{21}. \tag{37}$$

Let $\boldsymbol{e}_1, \boldsymbol{e}_2, \ldots, \boldsymbol{e}_M$ be the M eigenvectors of $\boldsymbol{E}$. We set $\boldsymbol{V}_1 = [\boldsymbol{e}_1, \boldsymbol{e}_2, \ldots, \boldsymbol{e}_{\frac{M}{2}}]$. Then $\boldsymbol{V}_2$ and $\boldsymbol{V}_3$ are found using (28)∼(30).

Similar to the derivation in Section II, the ZF filtering matrix at the first receiver is formulated as follows:

$$\boldsymbol{W}_1^{\text{ZF}} = \boldsymbol{\Psi}_1 \widetilde{\boldsymbol{H}}_1^{-1}, \tag{38}$$

where $\boldsymbol{\Psi}_1 = [\boldsymbol{I}_{\frac{M}{2}}, \boldsymbol{0}_{\frac{M}{2}}]$ and $\widetilde{\boldsymbol{H}}_1 = [\boldsymbol{H}_{11}\boldsymbol{V}_1, \boldsymbol{H}_{12}\boldsymbol{V}_2]$.

For the other receivers $k = 2, 3$, the ZF filtering matrix can be expressed as

$$\boldsymbol{W}_k^{\text{ZF}} = \boldsymbol{\Psi}_k \widetilde{\boldsymbol{H}}_k^{-1}, \tag{39}$$

where $\boldsymbol{\Psi}_k = [\boldsymbol{I}_{\frac{M}{2}}, \boldsymbol{0}_{\frac{M}{2}}]$ and $\widetilde{\boldsymbol{H}}_k = [\boldsymbol{H}_{kk}\boldsymbol{V}_k, \boldsymbol{H}_{k1}\boldsymbol{V}_1]$.

Applying the ZF receivers given by (38) and (39) to the received signal of (28), the average sum rate achieved by IA in the three-user multi-antenna interference channel is then given by

$$\overline{R}^* = \sum_{k=1}^{K} \log_2 \left| \boldsymbol{I}_{\frac{M}{2}} + \frac{P_k \boldsymbol{I}_{\frac{M}{2}}}{\boldsymbol{W}_k^{\text{ZF}} (\boldsymbol{W}_k^{\text{ZF}})^H} \right| \tag{40}$$

[bits per channel use]. Correspondingly, the EE expression is given by replacing $\bar{R}$ in (23) with $\overline{R}^*$ of (40).

B. THE EE OF IA FOR ODD-VALUED M

When M takes an odd value, to achieve a total of $3M/2$ DoF per channel use in the three-user interference channel, a two-symbol extension of the channel assuming constant channel coefficients over the duration of two symbols is needed, as shown in Fig. 3. Specifically, we have

$$\overline{\boldsymbol{y}}_k = \overline{\boldsymbol{H}}_{k1}\overline{\boldsymbol{V}}_1\boldsymbol{x}'_1 + \overline{\boldsymbol{H}}_{k2}\overline{\boldsymbol{V}}_2\boldsymbol{x}'_2 + \overline{\boldsymbol{H}}_{k3}\overline{\boldsymbol{V}}_3\boldsymbol{x}'_3 + \overline{\boldsymbol{z}}_k, \tag{41}$$

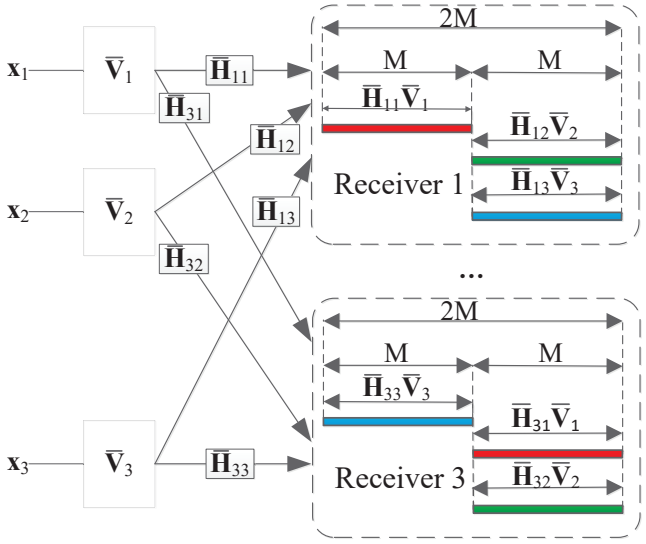

FIGURE 3. The IA scheme [5] where each node has an odd number of multiple antennas.

where $\overline{\boldsymbol{y}}_k$ and $\overline{\boldsymbol{z}}_k$ represent the two-symbol extension of the received signal $\boldsymbol{y}_k$ and of the noise vector $\boldsymbol{z}_k$ at the kth receiver, respectively. Furthermore, $\overline{\boldsymbol{H}}_{kj}$ is a $2M \times 2M$ block-diagonal matrix representing the extension of the channel, i.e., we have

$$\overline{\boldsymbol{H}}_{kj} = \begin{bmatrix} \boldsymbol{H}_{kj}(1) & \boldsymbol{0} \\ \boldsymbol{0} & \boldsymbol{H}_{kj}(1) \end{bmatrix}, j = 1, 2, 3. \tag{42}$$

Still referring to (41), $\overline{\boldsymbol{V}}_k \in \mathbb{C}^{2M\times M}$ is the precoding matrix invoked by the individual transmitters, and $\boldsymbol{x}'_k \sim \mathcal{CN}(\boldsymbol{0}, P_k \boldsymbol{I}_M)$ is an $M \times 1$ vector representing M independent data streams.

Similar to the even-M case, the following equations ensure that the interference at each of the receivers is aligned:

$$\text{span}(\overline{\boldsymbol{H}}_{12}\overline{\boldsymbol{V}}_2) = \text{span}(\overline{\boldsymbol{H}}_{13}\overline{\boldsymbol{V}}_3), \tag{43}$$
$$\overline{\boldsymbol{H}}_{21}\overline{\boldsymbol{V}}_1 = \overline{\boldsymbol{H}}_{23}\overline{\boldsymbol{V}}_3, \tag{44}$$
$$\overline{\boldsymbol{H}}_{31}\overline{\boldsymbol{V}}_1 = \overline{\boldsymbol{H}}_{32}\overline{\boldsymbol{V}}_2. \tag{45}$$

The above equations imply that

$$\text{span}(\overline{\boldsymbol{V}}_1) = \text{span}(\overline{\boldsymbol{E}}\,\overline{\boldsymbol{V}}_1), \tag{46}$$
$$\overline{\boldsymbol{V}}_2 = \overline{\boldsymbol{F}}\,\overline{\boldsymbol{V}}_1, \tag{47}$$
$$\overline{\boldsymbol{V}}_3 = \overline{\boldsymbol{G}}\,\overline{\boldsymbol{V}}_1, \tag{48}$$

where $\overline{\boldsymbol{E}}$, $\overline{\boldsymbol{F}}$ and $\overline{\boldsymbol{G}}$ are $2M \times 2M$ block-diagonal matrices representing the two-symbol extension of $\boldsymbol{E}$, $\boldsymbol{F}$ and $\boldsymbol{G}$, respectively. Hence, $\overline{\boldsymbol{E}}$, $\overline{\boldsymbol{F}}$ and $\overline{\boldsymbol{G}}$ are obtained by replacing $\boldsymbol{H}$ in (35) ∼ (37) with $\overline{\boldsymbol{H}}$, respectively.

Let $\boldsymbol{e}_1, \boldsymbol{e}_2, \ldots, \boldsymbol{e}_M$ be the eigenvectors of $\boldsymbol{E}$. Then, $\overline{\boldsymbol{V}}_1$ can be constructed as

$$\overline{\boldsymbol{V}}_1 = \begin{bmatrix} \boldsymbol{e}_1 & \boldsymbol{0} & \boldsymbol{e}_3 & \ldots & \boldsymbol{0} & \boldsymbol{e}_M \\ \boldsymbol{0} & \boldsymbol{e}_2 & \boldsymbol{0} & \ldots & \boldsymbol{e}_{M-1} & \boldsymbol{e}_M \end{bmatrix}. \tag{49}$$

Finally, $\overline{\boldsymbol{V}}_2$ and $\overline{\boldsymbol{V}}_3$ are determined by using (46)∼(48).

Again, the ZF filtering matrix at the first receiver is formulated as follows:

$$\overline{\boldsymbol{W}}_1^{\mathrm{ZF}} = \overline{\boldsymbol{\Psi}}_1 \overline{\widetilde{\boldsymbol{H}}}_1^{-1}, \tag{50}$$

where $\overline{\boldsymbol{\Psi}}_1 = [\boldsymbol{I}_M, \boldsymbol{0}_M]$ and $\overline{\widetilde{\boldsymbol{H}}}_1 = [\overline{\boldsymbol{H}}_{11}\overline{\boldsymbol{V}}_1, \overline{\boldsymbol{H}}_{12}\overline{\boldsymbol{V}}_2]$.

For the other receivers $k = 2, 3$, the ZF filtering matrix can be expressed as

$$\overline{\boldsymbol{W}}_k^{\mathrm{ZF}} = \overline{\boldsymbol{\Psi}}_k \overline{\widetilde{\boldsymbol{H}}}_k^{-1}, \tag{51}$$

where $\overline{\boldsymbol{\Psi}}_k = [\boldsymbol{I}_M, \boldsymbol{0}_M]$ and $\overline{\widetilde{\boldsymbol{H}}}_k = [\overline{\boldsymbol{H}}_{kk}\overline{\boldsymbol{V}}_k, \overline{\boldsymbol{H}}_{k1}\overline{\boldsymbol{V}}_1]$.

Applying the ZF receivers given by (50) and (51) to the received signal of (41), the average sum rate achieved by IA in the three-user interference channel is then given by

$$R_k = \frac{1}{2}\sum_{k=1}^{K} \log_2 \left| \boldsymbol{I}_M + \frac{P_k \boldsymbol{I}_M}{\overline{\boldsymbol{W}}_k^{\mathrm{ZF}} \left(\overline{\boldsymbol{W}}_k^{\mathrm{ZF}}\right)^H} \right| \tag{52}$$

[bits per channel use]. The corresponding EE expression is given by replacing $\bar{R}$ in (23) with R_k of (52).

IV. ANALYSIS OF COMPUTATIONAL COMPLEXITY

Most of the existing literature related to the computational complexity of IA, such as [26], [27], were focused on the distributed IA scheme proposed in [28]. It was proved in [26], [27] that the sum DoF maximization problem and the DoF achievability problem are both NP-hard if each transmitter/receiver has at least three antennas.

By contrast, the IA schemes studied in this paper obtain the precoding matrices and the ZF filtering matrices through direct analysis and derivation, rather than through the iteration process of [28]. Thus, the computational complexity of the IA schemes studied herein is mainly related to matrix multiplication. In this paper, since the matrix multiplications from (6) to (10) use diagonal matrices, the computational complexity of this part is $\mathcal{O}(M_e)$. The computational complexity of (17) and (18) is $\mathcal{O}(D_{sum}M_e^2)$, where D_{sum} denotes the sum of achievable DoF for all users. As a result, the complexity of the IA schemes considered in this paper is $\mathcal{O}(M_e) + \mathcal{O}(D_{sum}M_e^2) = \mathcal{O}(D_{sum}M_e^2)$.

Note that D_{sum} and M_e are obtained in different ways for the two IA schemes studied. In the canonical IA scheme of [5], $D_{sum} = (n+1)^N + (K-1)n^N$ and M_e is given by (3). In the efficient IA scheme of [24], $D_{sum} = \binom{n^*+N+1}{N} + (K-1)\binom{n^*+N}{N}$ and M_e is given by (13). It is clear that the IA scheme of [24] has an advantage in terms of computational complexity over the IA scheme of [5].

V. SIMULATION RESULTS AND DISCUSSIONS

In this section, simulation results are provided to illustrate the EE performance of the canonical IA scheme [5], the IA scheme [24] and their respective variants in both the perfect and imperfect CSI scenarios, where the ZF receiver is employed. These variants are different from their respective baseline schemes in terms of the precoding-matrix-generating vector, the length of symbol extension, or the power allocation strategy. For the single-antenna case of the canonical IA of [5] and its corresponding improved scheme, we consider $(K, n) \in \{(3,1), (3,5), (4,1), (4,2), (5,1)\}$, which results in $M_e = \{3, 11, 33, 275, 2049\}$, respectively using (3). For the single-antenna case of the IA scheme of [24] and its corresponding improved scheme, we consider $(K, n^*) \in \{(3,0), (3,1), (4,0), (4,1), (5,0), (5,1)\}$, which results in $M_e = \{3, 5, 7, 27, 13, 90\}$, respectively using (13). For the multi-antenna case, we consider $M = 2, 3, 4, 5$. We use $\boldsymbol{w}_1 = 1$ to indicate that an all-one precoding-matrix-generating vector $\boldsymbol{w}$ is used, and $\boldsymbol{w}_1 = 4$ to indicate that the first element of the precoding-matrix-generating vector $\boldsymbol{w}$ is changed to 4, while the remaining elements of the precoding-matrix-generating vector $\boldsymbol{w}$ are still one. Having a unit noise variance of $\sigma^2 = 1$ is assumed.

In Fig. 4, we show the average achievable EE of the canonical IA scheme [5], the IA scheme [24], and their respective variants in the perfect CSI scenario with single-antenna nodes. We consider $K = 3, 4, 5$ users, different values of M_e [calculated using (K, n) and (K, n^*) according to (3) and (13), respectively, and also given in the above paragraph for convenience], different precoding-matrix-generating vectors (indicated by $\boldsymbol{w}_1$) and different transmit power allocation schemes (indicated by the values of $\chi_1, \cdots, \chi_K$).

We observe from Fig. 4 that the IA scheme [24] relying on an improved precoding matrix design criterion achieves higher EE than that of the canonical IA scheme [5] in the entire $\mathrm{SNR}_{\mathrm{Tx}} = P_t/\sigma^2$ region, when they use the same precoding-matrix-generating vector (e.g., $\boldsymbol{w}_1 = 1$) and the same transmit power allocation scheme (e.g., equal power allocation) in the scenario of $K \geq 4$.

Moreover, Fig. 4 shows that the EE performance changes when using different precoding-matrix-generating vectors. Specifically, comparing the green solid (or red dashed) curve having the marker of square with the curve of the IA scheme [5] (or [24]) in each subfigure of Fig. 4, we see that the variant schemes exhibit an inferior EE performance, when invoking the precoding-matrix-generating vector $\boldsymbol{w}_1 = 4$ rather than $\boldsymbol{w}_1 = 1$ used by the IA schemes [5] and [24]. However, this degradation is reduced when increasing K.

Furthermore, in Fig. 4 by comparing the curves of the IA scheme [5] (or [24]) with the green solid (or red dashed) curves having the marker of diamond, we find that the EE performance of IA with smaller symbol extension values (indicated here by lower n and n^*) is higher than that with larger symbol extension values, while using a certain transmit power allocation scheme in the whole $\mathrm{SNR}_{\mathrm{Tx}}$ region.

Additionally, by comparing the green solid (or red dashed) curves having the marker of triangle with that of the IA scheme [5] (or [24]) in Fig. 4, we observe that an unequal transmit power allocation strategy with χ_1 having a larger value results in a higher EE performance than the equal power allocation strategy in the IA schemes considered. It should also be pointed out that the EE decreases upon increasing the total transmit power (indicated by $\mathrm{SNR}_{\mathrm{Tx}} = P_t/\sigma^2$) in all scenarios considered. Notably, the EE ap-

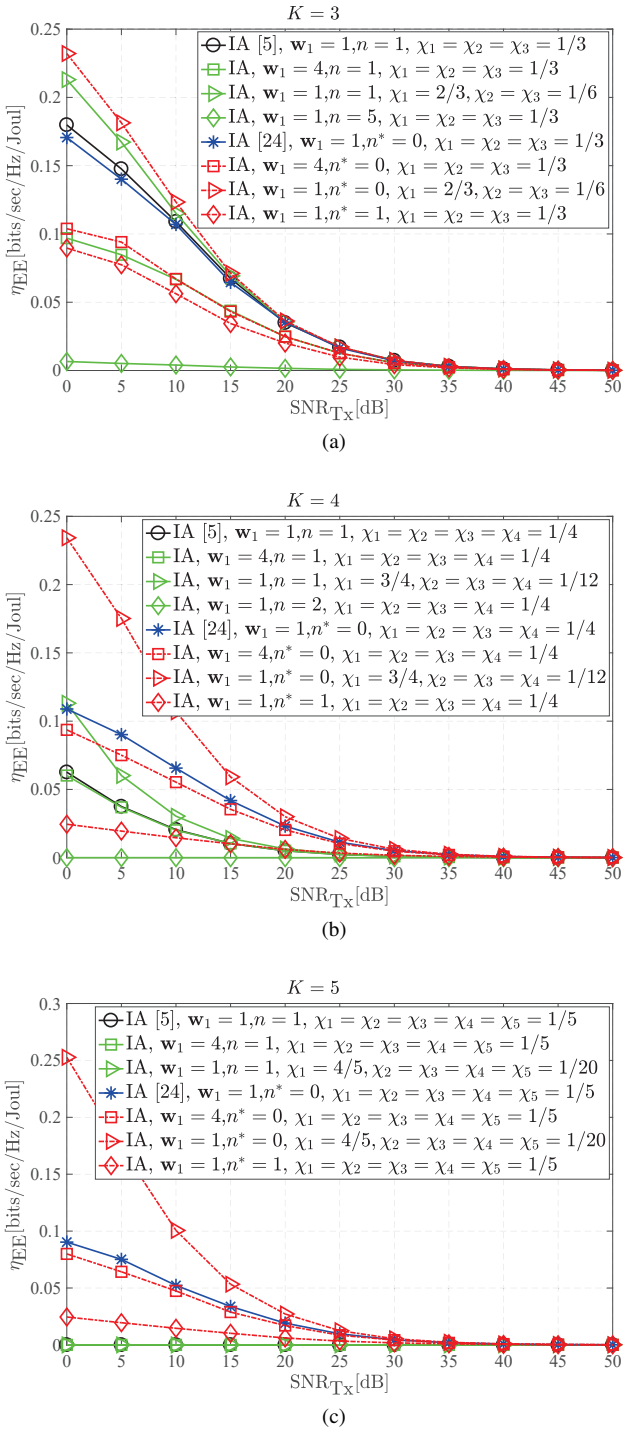

FIGURE 4. The average achievable EE of $K = 3$ (a), $K = 4$ (b), $K = 5$ (c) users utilizing the canonical IA scheme [5], the IA scheme [24], and their respective variants in the perfect CSI scenario with single-antenna nodes. Different values of symbol extension, different precoding-matrix-generating vectors and different transmit power allocation schemes are considered.

proaches zero with sufficiently high $\mathrm{SNR}_{\mathrm{Tx}}$ values. The reason is as follows. With the increasing $\mathrm{SNR}_{\mathrm{Tx}}$, the average sum rate achieved by the IA scheme grows in a slow "log" manner according to (20) and (21), while the total power dissipation $P = P_t + P_c$ of the system grows in a faster "linear" manner. As a result, the EE approaches zero as the $\mathrm{SNR}_{\mathrm{Tx}}$ tends to a sufficiently large value, according to (23). This result implies that although increasing the $\mathrm{SNR}_{\mathrm{Tx}}$ can always increase the sum rate, the sum-rate return corresponding to per-Joule energy investment is diminishing from the EE perspective.

The impact of channel estimation accuracy on the EE of the canonical IA scheme [5] is illustrated in Fig. 5 for the single-antenna case. We consider both 3-user and 4-user interference channels with $M_e = 3$ and $M_e = 33$ symbol extension at $\mathrm{SNR}_{\mathrm{Tx}} = 5$ dB, respectively. Both cases are evaluated by using different power allocation schemes and different precoding-matrix-generating vectors. We observe that the average EE performance degrades as the channel estimation accuracy indicator β increases. The EE remains almost constant when β is lower than 10^{-3}. When β approaches one (i.e., $\lg(\beta^2)$ approaches zero), the EE rapidly degrades. We also observe that the EE of $K = 3$ is higher than that of $K = 4$, assuming the same channel estimation accuracy, the same power allocation scheme and the same precoding-matrix-generating vectors.

Fig. 6 shows the impact of the number of antennas M and different transmit power allocation schemes on the average achievable EE of IA. We observe that a larger M achieves a higher EE. However, it indicates that the IA scheme [5] relying on the equal power allocation of $\chi_1 = \chi_2 = \chi_3 = 1/3$ outperforms the variant IA scheme relying on the unequal power allocation of $\chi_1 = 2/3, \chi_2 = 1/6, \chi_3 = 1/6$ with the same value of M in terms of the EE. Note that this observation is different from that of the single-antenna-user case. The reason is as follows. In the MIMO case, all users equally share the DoF, whilst in the single-antenna-user case considered, the user 1 has a larger DoF than the other users. Similar to the results of Fig. 4, the achievable EE of the multi-antenna scenario decays with the total transmit power.

VI. CONCLUSIONS

We have investigated the EE of IA in the fully connected single-antenna and multi-antenna K-user interference channels. We derive the EE expression of IA considering both perfect and imperfect CSI scenarios. New insights into the achievable EE of IA are obtained by investigating the impact of different precoding matrices, the number of users, symbol extension values, the number of antennas, channel estimation accuracy, total transmit power and power allocation schemes. In particular, we demonstrate that in the single-antenna-user case, the IA schemes relying on unequal power allocation achieves higher EE than their equal power allocation counterparts. However, in the scenario where each user is equipped with multiple antennas, equal power allocation achieves higher EE than unequal power allocation for IA. Furthermore, using non-uniform precoding-matrix-generating vector $\boldsymbol{w}$ is not necessarily beneficial for improving the achievable EE of IA. We also find that the EE performance of IA with smaller symbol extension values is higher than that with larger symbol extension values, the

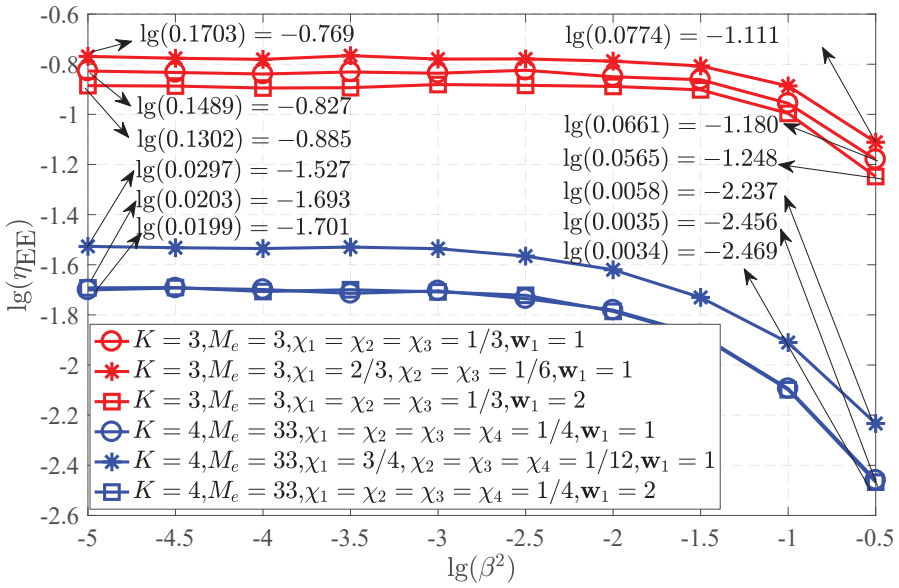

FIGURE 5. The impact of channel estimation accuracy on the average achievable EE of the canonical IA scheme of [5]. We consider 3-user and 4-user single-antenna interference channels with $M_e = 3$ and $M_e = 33$ symbol extension at $\mathrm{SNR}_{\mathrm{Tx}} = 5$ dB, respectively. Both cases are evaluated by using different power allocation schemes and different precoding-matrix-generating vectors.

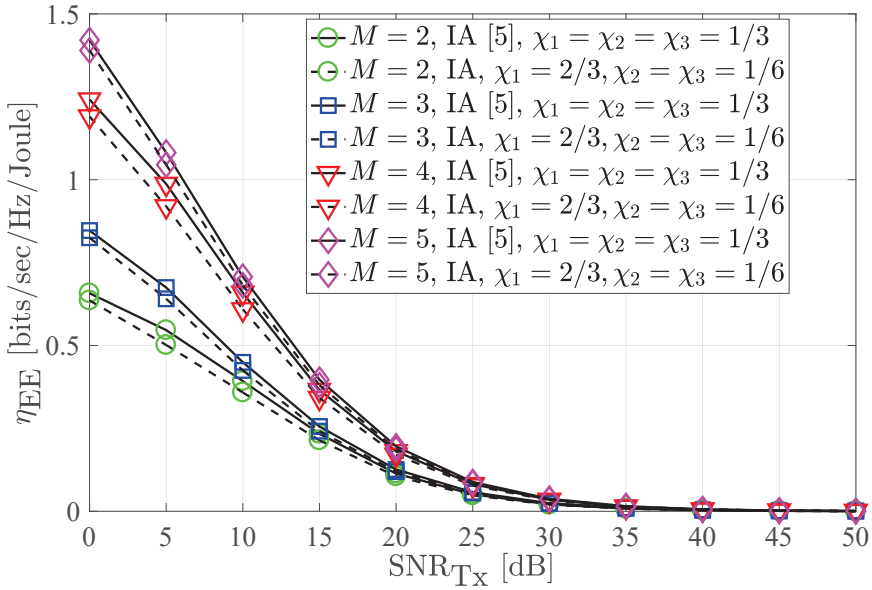

FIGURE 6. The average achievable EE of the canonical IA scheme [5] with equal transmit power allocation and of the variant IA scheme with unequal transmit power allocation, considering a 3-user interference channel with each user having $M > 1$ transmitting/receiving antennas. Perfect CSI and different values of the number of antennas are considered.

EE performance of IA degrades as the channel estimation accuracy become low, and that having a larger number of transmit/receive antennas on each user achieves a higher EE in IA. Finally, the achievable EE of IA decays with the increase of the total transmit power. In our future work, we will study the design of optimal IA schemes that are capable of maximizing the achievable EE.

REFERENCES

[1] M. A. Maddah-Ali, A. S. Motahari, and A. K. Khandani, "Signaling over MIMO multi-base systems: combination of multi-access and broadcast schemes," in Proc. IEEE Int. Symp. Inf. Theory (ISIT'06), Seattle, WA, Jul. 2006, pp. 2104–2108.

[2] ——, "Communication over X channel: signalling and multiplexing gain," Department of Electrical and Computer Engineering, University of Waterloo, Waterloo, ON, Canada, Tech. Rep. UW-ECE-2006-12, Jul. 2006.

[3] ——, "Communication over MIMO X channel: signalling and perfor-

mance analysis," Department of Electrical and Computer Engineering, University of Waterloo, Waterloo, ON, Canada, Tech. Rep. UW-ECE-2006-27, Dec. 2006.
[4] ——, "Communication over MIMO X channels: interference alignment, decomposition, and performance analysis," IEEE Trans. Inf. Theory, vol. 54, no. 8, pp. 3457–3470, Aug. 2008.
[5] V. Cadambe and S. Jafar, "Interference alignment and degrees of freedom of the K-user interference channel," IEEE Trans. Inf. Theory, vol. 54, no. 8, pp. 3425–3441, Aug. 2008.
[6] S. A. Jafar, "Interference alignment – a new look at signal dimensions in a communication network," Foundations and Trends in Communications and Information Theory, vol. 7, no. 1, 2010.
[7] S. M. Perlaza, N. Fawaz, S. Lasaulce, and M. Debbah, "From spectrum pooling to space pooling: Opportunistic interference alignment in MIMO cognitive networks," IEEE Trans. Signal Process., vol. 58, no. 7, pp. 3728–3741, Jul. 2010.
[8] V. Ntranos, M. A. Maddah-Ali, and G. Caire, "Cellular interference alignment," IEEE Trans. Inf. Theory, vol. 61, no. 3, pp. 1194–1217, March 2015.
[9] N. Zhao, F. R. Yu, H. Sun, and M. Li, "Adaptive power allocation schemes for spectrum sharing in interference-alignment-based cognitive radio networks," IEEE Trans. Veh. Technol., vol. 65, no. 5, pp. 3700–3714, May. 2016.
[10] N. Zhao, S. Zhang, F. R. Yu, Y. Chen, A. Nallanathan, and V. C. M. Leung, "Exploiting interference for energy harvesting: A survey, research issues, and challenges," IEEE Access, vol. 5, pp. 10 403–10 421, 2017.
[11] L. Zheng and D. N. C. Tse, "Diversity and multiplexing: A fundamental tradeoff in multiple-antenna channels," IEEE Trans. Inf. Theory, vol. 49, no. 5, pp. 1073–1096, May. 2003.
[12] C. Han, T. Harrold, S. Armour, I. Krikidis, S. Videv, P. M. Grant, H. Haas, J. S. Thompson, I. Ku, C.-X. Wang, T. A. Le, M. R. Nakhai, J. Zhang, and L. Hanzo, "Green radio: Radio techniques to enable energy-efficient wireless networks," IEEE Commun. Mag., vol. 49, no. 6, pp. 46–54, Jun. 2011.
[13] Y. Chen, S. Zhang, S. Xu, and G. Y. Li, "Fundamental trade-offs on green wireless networks," IEEE Commun. Mag., vol. 49, no. 6, pp. 30–37, Jun. 2011.
[14] J. Hoydis, M. Kobayashi, and M. Debbah, "Green small-cell networks," IEEE Veh. Technol. Mag., vol. 6, no. 1, pp. 37–43, Mar. 2011.
[15] K. T. K. Cheung, S. Yang, and L. Hanzo, "Achieving maximum energy-efficiency in multi-relay OFDMA cellular networks: A fractional programming approach," IEEE Trans. Commun., vol. 61, no. 7, pp. 2746–2757, Jul. 2013.
[16] ——, "Spectral and energy spectral efficiency optimization of joint transmit and receive beamforming based multi-relay MIMO-OFDMA cellular networks," IEEE Trans. Wireless Commun., vol. 13, no. 11, pp. 6147–6165, Nov. 2014.
[17] T. Abrão, L. Sampaio, S. Yang, K. T. K. Cheung, P. J. E. Jeszensky, and L. Hanzo, "Energy efficient OFDMA networks maintaining statistical QoS guarantees for delay-sensitive traffic," IEEE Access, vol. 4, Mar. 2016.
[18] W. Jing, Z. Lu, X. Wen, Z. Hu, and S. Yang, "Flexible resource allocation for joint optimization of energy and spectral efficiency in ofdma multi-cell networks," IEEE Commun. Lett., vol. 19, no. 3, pp. 451–454, March 2015.
[19] F. Tan, T. Lv, and S. Yang, "Power allocation optimization for energy-efficient massive mimo aided multi-pair decode-and-forward relay systems," IEEE Trans. Commun., vol. 65, no. 6, pp. 2368–2381, June 2017.
[20] J. Yoon, W. Y. Shin, and H. S. Lee, "Energy-efficient opportunistic interference alignment," IEEE Commun. Lett., vol. 18, no. 18, pp. 30–33, Jan. 2014.
[21] N. Zhao, F. R. Yu, and H. Sun, "Adaptive energy-efficient power allocation in green interference-alignment-based wireless networks," IEEE Trans. Veh. Technol., vol. 64, no. 9, pp. 4268–4281, Sep. 2015.
[22] K. T. K. Cheung, S. Yang, and L. Hanzo, "Distributed energy spectral efficiency optimization for partial/full interference alignment in multi-user multi-relay multi-cell MIMO systems," IEEE Trans. Signal Process., vol. 64, no. 4, pp. 882–896, Feb. 2016.
[23] J. Tang, D. K. C. So, E. Alsusa, and K. A. Hamdi, "Energy efficiency optimization with interference alignment in multi-cell MIMO interfering broadcast channels," IEEE Trans. Commun., vol. 63, no. 7, pp. 2486–2499, Jul. 2015.
[24] S. W. Choi, S. A. Jafar, and S. Y. Chung, "On the beamforming design for efficient interference alignment," IEEE Commun. Lett., vol. 13, no. 11, pp. 847–849, Nov. 2009.
[25] C. Wang, E. K. S. Au, R. D. Murch, W. H. Mow, R. S. Cheng, and V. Lau, "On the performance of the MIMO zero-forcing receiver in the presence of channel estimation error," IEEE Trans. Wireless Commun., vol. 6, no. 3, pp. 805–810, Mar. 2007.
[26] M. Razaviyayn, M. Sanjabi, and Z. Luo, "Linear transceiver design for interference alignment: Complexity and computation," IEEE Trans. Inf. Theory, vol. 58, no. 5, pp. 2896–2910, May 2012.
[27] L. Ma, T. Xu, and G. Sternberg, "Computational complexity of interference alignment for symmetric MIMO networks," IEEE Commun. Lett., vol. 17, no. 12, pp. 2308–2311, Dec. 2013.
[28] K. Gomadam, V. R. Cadambe, and S. A. Jafar, "A distributed numerical approach to interference alignment and applications to wireless interference networks," IEEE Trans. Inf. Theory, vol. 57, no. 6, pp. 3309–3322, Jun. 2011.

XIAQING MIAO received the B.S. degree in logistics engineering from the Beijing University of Posts and Telecommunications, Beijing, P. R. China in 2012. He is currently pursuing the Ph.D. degree at the Beijing Institute of Technology, Beijing, P. R. China. Since October 2017, he has been with the Department of Electrical Engineering and Computer Science, Northwestern University, Evanston, IL, USA, where he is a visiting Ph.D. student under the supervision of Prof. Dongning Guo. His research interests include wireless communication and signal processing.

SHAOSHI YANG (S'09-M'13-SM'19) received the B.Eng. degree in information engineering from Beijing University of Posts and Telecommunications (BUPT), China in 2006, and the Ph.D. degree in electronics and electrical engineering from University of Southampton, U.K. in 2013. From 2008 to 2009, he was involved in the WiMAX standardization with Intel Labs China. From 2013 to 2016, he was a Research Fellow with the School of Electronics and Computer Science, University of Southampton. From 2016 to 2018, he was a Principal Engineer with Huawei Technologies Co., Ltd., where he led the company's research efforts in wireless video/VR transmission. Currently, he is a Full Professor at BUPT. His research expertise include 4G/5G wireless networks, massive MIMO signal processing, iterative signal processing, cross-layer design, wireless AI, and wireless video/AR/VR. He received the Dean's Award for Early Career Research Excellence from the University of Southampton in 2015, the President Award of Wireless Innovations from Huawei in 2018, and the IEEE Technical Committee on Green Communications & Computing (TCGCC) Best Journal Paper Award in 2019. He is a member of the Isaac Newton Institute for Mathematical Sciences, Cambridge University, and an Editor for IEEE Wireless Communications Letters. He was also an invited international reviewer for the Austrian Science Fund (FWF). (http://shaoshiyang.weebly.com/)

CHANGHONG WANG received the B.S. degree in communication engineering from Zhengzhou University, China in 2013, and is currently pursuing the Ph.D. degree in information and communication engineering at the Beijing Institute of Technology, China. His main research interests include spread spectrum communication, anti-jamming transmission, and digital signal processing. He has contributed to the design and testing of two ASICs, which implements the function of spread spectrum transmitter and receiver.

SHUAI WANG received his B.Eng. degree and Ph.D. degree from Zhengzhou University and Beijing Institute of Technology, P. R. China, in 2005 and 2012 respectively, both in communications engineering, and both with the highest honor. He won the "Outstanding Ph.D. Dissertation" award granted by the Beijing Municipal Education Commission in 2013 with other 49 co-winners, nominated from all the Ph.D. graduates who received their degree in Beijing that year. From September 2010 to September 2011 he was a visiting Ph.D. student in the School of Electronics and Computer Science, University of Southampton, U.K. He has been with the School of Information Science and Electronics, Beijing Institute of Technology since July 2012, where he is now an Associate Professor. His research interests include channel estimation, anti-jamming transmission, synchronization techniques and beamforming. He has published more than 30 peer-reviewed articles, mainly in IEEE journals or conferences. Prof. Wang served or is serving as the Principal Investigator for 12 research projects, including two granted by the National Science Foundation of China. He is a recipient of the (Second Class) Scientific and Technological Progress Award granted by the Ministry of Industry and Information Technology of China. He also holds 20 patents. He is a member of the Editorial Board of China Communications, sponsored by the China Institute of Communications (CIC).

LAJOS HANZO (M'91–SM'92–F'04) (FREng, FIEEE, FIET, FEURASIP, DSc) received his degree in electronics in 1976 and his doctorate in 1983. In 2009 he was awarded an honorary doctorate by the Technical University of Budapest and in 2015 by the University of Edinburgh. In 2016 he was admitted to the Hungarian Academy of Science. During his 43-year career in telecommunications he has held various research and academic posts in Hungary, Germany and UK. Since 1986 he has been with the School of Electronics and Computer Science, University of Southampton, UK, where he holds the chair in telecommunications. He has successfully supervised more than 110 PhD students, co-authored 20 John Wiley/IEEE Press books on mobile radio communications totalling in excess of 10 000 pages, published 1400+ research contributions at IEEE Xplore, acted both as TPC and General Chair of IEEE conferences, presented keynote lectures and has been awarded a number of distinctions. Currently he is directing a 60-strong academic research team, working on a range of research projects in the field of wireless multimedia communications sponsored by industry, the Engineering and Physical Sciences Research Council (EPSRC) UK, the European Research Council's Advanced Fellow Grant and the Royal Society's Wolfson Research Merit Award. He is an enthusiastic supporter of industrial and academic liaison and he offers a range of industrial courses. He is also a Governor of the IEEE VTS. During 2008–2012 he was the Editor-in-Chief of the IEEE Press and also a Chaired Professor at Tsinghua University, Beijing. Lajos has 43000+ citations and an H-index of 81 on Google Scholar. For further information on research in progress and associated publications please refer to http://www-mobile.ecs.soton.ac.uk.